NASA TECHNICAL NOTE

NASA TN D-4380

NASA TN D-4380

PERFORMANCE STUDY OF ROTATING GAS JET GENERATOR FOR STRONG TRAVELING TRANSVERSE ACOUSTIC MODES

by Marcus F. Heidmann

Lewis Research Center
Cleveland, Ohio

NATIONAL AERONAUTICS AND SPACE ADMINISTRATION • WASHINGTON, D. C. • FEBRUARY 1968

PERFORMANCE STUDY OF ROTATING GAS JET GENERATOR FOR STRONG TRAVELING TRANSVERSE ACOUSTIC MODES

By Marcus F. Heidmann

Lewis Research Center
Cleveland, Ohio

NATIONAL AERONAUTICS AND SPACE ADMINISTRATION

For sale by the Clearinghouse for Federal Scientific and Technical Information
Springfield, Virginia 22151 – CFSTI price $3.00

PERFORMANCE STUDY OF ROTATING GAS JET GENERATOR FOR STRONG TRAVELING TRANSVERSE ACOUSTIC MODES

by Marcus F. Heidmann

Lewis Research Center

SUMMARY

An experimental investigation is made of a traveling transverse acoustic mode generator which utilizes a rotating gas jet as an energy source. The gas jet is radially alined and located at the center of a short cylindrical cavity with an exhaust port at the center of one end plate. Jet rotation is varied over a range of speeds encompassing the rotational speeds of several "spinning" transverse acoustic modes and pressure amplitudes are measured at the circumference of the cavity. The effect of jet total pressure, jet configuration, and cavity diameter on amplitude is investigated.

Pressure amplitude as a function of rotational speed for a single radial jet exhibits several conditions of resonance. One occurs when jet speed corresponds to the resonant frequency of the first transverse mode. Higher modes occur at lower rotational speeds where more than one pressure oscillation is obtained for each rotation of the jet. For all modes and jet configurations, pressure amplitudes increase with an increase in jet total pressure and flow rate. Maximum peak-to-peak pressure amplitudes for all conditions was 38 psi (2.62×10^5 N/m^2) which corresponds to a sound pressure level of 192 decibels. The wave shape at all resonant conditions was symetrical with time about the peak pressure and appeared free of shocks.

The conversion efficiency of potential jet power to acoustic power was evaluated for all resonant conditions. In general, efficiency increased with an increase in jet total pressure. A maximum efficiency of 44 percent was observed with a divergent nozzle. Small diameter jets in a large diameter cavity generally gave highest efficiencies; however, the result depends on jet total pressure. Two radial jets gave improved efficiencies over a single jet in generating the second transverse mode. Efficiencies for the higher modes, however, were nearly an order of magnitude lower than for the first mode for each increase in mode number.

INTRODUCTION

This report presents a performance evaluation of an acoustic generator which produces strong traveling transverse resonant modes in a cylindrical cavity. The generator consists of a radially directed gas jet which is rotated at the center of a short cylindrical cavity by an air turbine motor at speeds compatible with the transverse resonant frequencies of the cavity. The effect of rotational speed, jet flow rate, jet geometry, and cavity diameter on acoustic generation is evaluated and a performance analysis of the results is made.

The acoustic properties of strong traveling transverse modes differ from those of conventional "organ-pipe" modes in several respects. These modes have pure traveling properties at the circumference of the cavity giving maximum particle velocities at the time cavity pressure is at either a maximum or a minimum. In contrast, the particle velocity in standing type modes is a maximum when the oscillating cavity pressure attains the mean value. These oscillations also differ from organ pipe oscillation in that strong waves without shocks can be developed (ref. 1).

Traveling wave properties are frequently desired in test apparatus utilizing acoustic environments to study the dynamic behavior of physical and chemical phenomena. In particular, the effects of strong traveling oscillations on liquid propellant atomization, vaporization, and burning and on solid propellant erosion and burning are important to the study of combustion instability in chemical rockets because destructive oscillations are frequently associated with traveling modes. Similarly, the effect of traveling oscillations on the performance of acoustic absorbers, pressure transducers, and heat-transfer process is needed. Traveling modes are also encountered in other areas such as gas turbine combustion, axial-flow compressor noise generation, large duct airflow systems, etc. These encounters with traveling modes frequently necessitate that controlled oscillation be established so that the detailed behavior of a process or mechanism can be examined.

Traveling acoustic modes can be generated by various means. A conventional method (refs. 2 and 3) utilizes two oscillating energy sources (pistons, air choppers, etc.) angularly displaced about the circumference of a cylinder. The outputs of the two sources are phased to produce traveling oscillations. One limitation of oscillating mechanical or aerodynamic sources is that inertia effects frequently restrict the output at high frequencies or create impractical demands on input power. The continuous flow process used in this study minimizes these inertia limitations and eliminates the need for phase control of two sources. The primary limitation on the rotary jet-energy source is the control and generation of high rotational speeds. These limitations may be less restrictive than inertia effects in some applications, particularly when high power output or large installations are required.

TRAVELING TRANSVERSE ACOUSTIC MODES

Traveling transverse acoustic modes have the unique property of interchangeability of time and angular position. This is illustrated in figure 1 for the fundamental mode where the mode is described by a fixed pattern of isobars and velocity vectors which rotate once for each cycle of oscillation. The fixed pattern is more complex for harmonic modes (fig. 2) where the number of pressure lobes described by the isobars is proportional to the mode number. For these higher harmonic modes, a fixed position on the circumference experiences, in each rotation of the pattern, pressure oscillations proportional in number to the mode number.

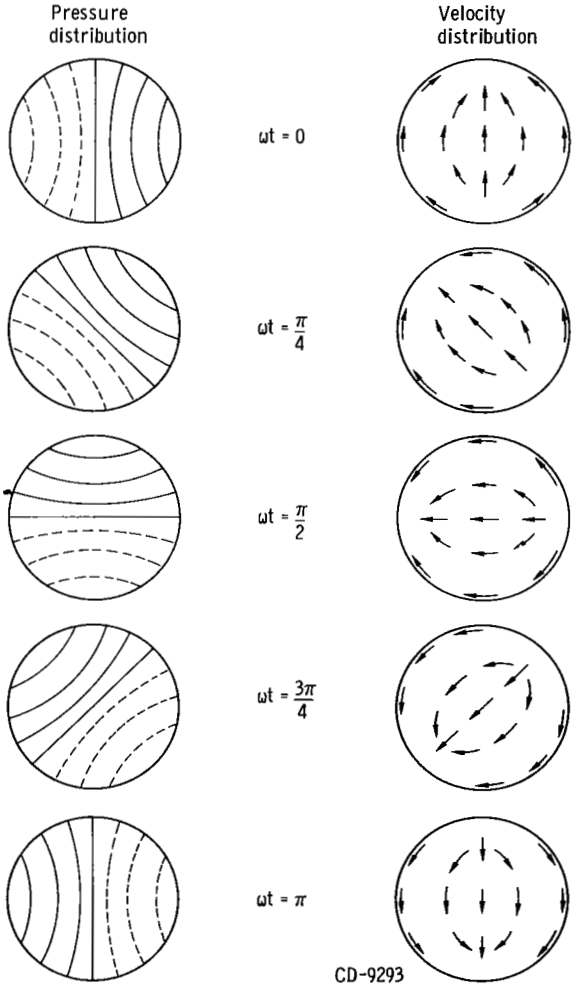

Figure 1. - Fundamental tangential mode: traveling wave form.

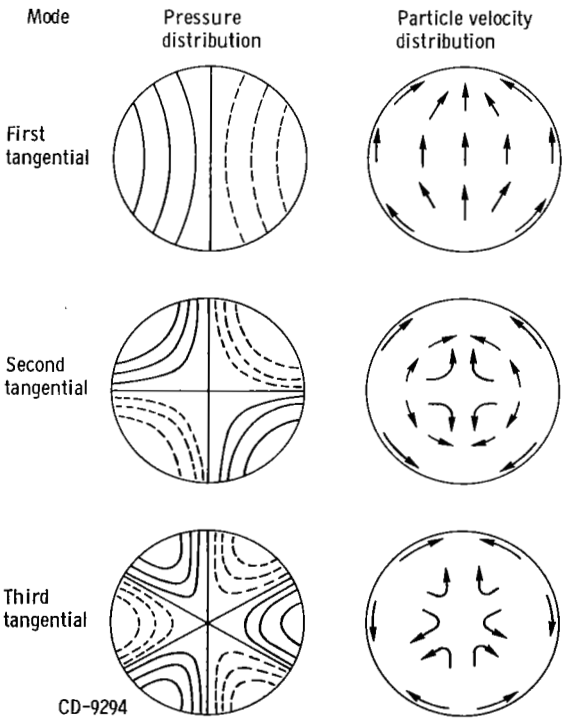

Figure 2. - Theoretical transverse modes: traveling wave form.

Analytically, the acoustic properties of these traveling modes are described to first order for inviscid flow (ref. 1) by

$$P = \bar{P}\left[1 - \epsilon\gamma J_n(\alpha)\cos(\omega t + n\theta)\right] \tag{1}$$

$$T = \bar{T}\left[1 - (\gamma - 1)\epsilon J_n(\alpha)\cos(\omega t + n\theta)\right] \tag{2}$$

$$\rho = \bar{\rho}\left[1 - \epsilon J_n(\alpha)\cos(\omega t + n\theta)\right] \tag{3}$$

$$u_\theta = \epsilon a_o n \frac{J_n(\alpha)}{\alpha} \cos(\omega t + n\theta) \tag{4}$$

$$u_r = \epsilon a_o \left[J_{n-1}(\alpha) - n\frac{J_n(\alpha)}{\alpha}\right]\sin(\omega t + n\theta) \tag{5}$$

(All symbols are defined in appendix A.)

The first order expression for the oscillation frequency of these traveling modes is given by

$$f_n = B_n \frac{a_o}{2R} = nM_n \frac{a_o}{2\pi R} \tag{6}$$

where the values of n, B_n, and M_n are given in the following table:

n	B_n	M_n
1	0.586	1.84
2	.972	1.53
3	1.337	1.40
4	1.693	1.33

The factor B_n is obtained from a solution of the wave equations describing the mode (ref. 4). The factor M_n is the apparent Mach number or phase velocity of the traveling wave at the circumference of the cavity. It is seen that the rotational speed of the fixed pattern of isobars and velocity vectors decreases with an increase in mode number. In the extreme, the Mach number is one for an infinite mode number.

Strong or high amplitude oscillations require higher order solutions of the wave equations and a consideration of viscous dissipation to accurately describe acoustic properties, resonant frequencies, and wave shapes. High amplitude and viscous effects

have been investigated analytically in reference 1. The general results of reference 1 are as follows:

(1) "... the cylindrical mode cannot be regarded as a train of distinct pulses, but is rather an interference pattern in which the scattering effect of the wall overcomes any tendency for components to steepen into shocks such as occur in a plane mode of oscillation."

(2) "The amplitude variation of the finite potential wave is, for a cylindrical mode, symmetrical in both time and angle.... If the wall pressure in the first traveling transverse mode were plotted against $(\omega t + \theta)$, the resulting plot would be quite similar to that in [fig. 3]..."

(3) "The frequency is a function of wave amplitude, if the maximum peak-to-peak pressure amplitude in the first (lowest frequency) transverse mode is one-third the chamber pressure - i.e., about 176 decibels - the frequency of the strong wave is reduced from that of the associated sonic mode by less than 2 percent."

(4) A consideration of the boundary layer at the wall results in a classical phenomenon known as acoustic streaming. "For a traveling - i.e., spinning - wave, the second-order streaming exhibits a steady temperature perturbation and a steady wheel flow, but no pressure perturbation. The flow direction for practical modes is opposite to that of wave propagation...." Such wheel flow causes an additional reduction in frequency beyond that caused by potential flow considerations.

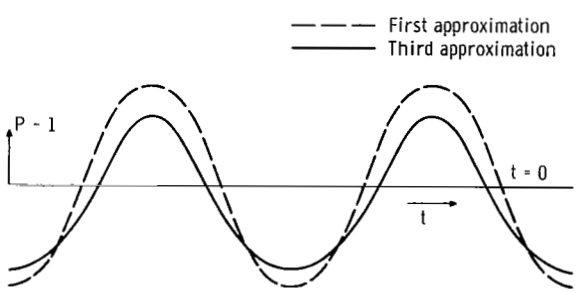

Figure 3. - Time variation of wall pressure wave shape (ref. 1).

DESCRIPTIVE MODEL

A model for acoustic amplification of traveling transverse modes by a rotating gas jet can be formulated from the foregoing considerations of the acoustic properties of such modes.

Assuming a cylindrical coordinate system which rotates with the speed of the wave, the acoustic wave may be visualized as a steady mass flow process (see figs. 1 and 2). The magnitude of this mass flow increases with an increase in wave amplitude

(eqs. (1) to (5)). Conversely, a process which can increase the mass flow might also increase the wave amplitude.

A gas jet at the center of a cylindrical mode and rotating at the speed of the wave can act to increase the mass flow associated with the acoustic mode. This is illustrated in figure 4 for the first transverse mode where the gas jet is alined with the direction of the mass flow. The action of the jet in this instance is similar to that of a jet in an air ejector. Mass, momentum, and energy of the jet flow can cause an acceleration of the acoustic mass flow. The magnitude of the acoustic amplification from such jet flow depends on a detailed knowledge of the path of the jet expansion and mixing process. As in the case of air ejectors, analytical solutions are generally inadequate because ideal processes cannot be postulated. Experimental evaluations are usually required. Some acoustic amplification or conversion of jet energy to acoustic energy, however, may be expected.

When a radial gas jet induces flow at the center of the cavity, rotating the jet at the speed of the first transverse mode will initiate such a mode of oscillation. The acoustic mode will increase in intensity at a rate depending on acoustic losses and gains. An exhaust port at the center of the cavity (fig. 4) or any other position in the cavity is a primary source of flow losses. Viscous dissipation within the cavity is also important as is the efficiency of the jet mixing process.

The flow processes for higher order acoustic modes are more complex. For example, a jet at the center of the second transverse mode (fig. 2) is not in a region of unidirectional flow. A degree of amplification may be expected, however, if the jet flow maintains an alinement with one of the velocity vectors emanating from the center. Acceleration of the flow field in the direction of the jet would be accompanied by some retardation of the flow field in the opposite direction. A typical jet mixing process would appear to favor a net increase in the flow, and generation of higher order modes with a single jet may be expected.

Higher order modes generated by a single jet require lower jet rotational speeds than for the fundamental or first mode. The rotational speed of the mode decreases with an increase in mode number (eq. (6)). The jet rotation speed would be f_n/n.

A more efficient flow process for higher order modes can be visualized when more than one jet ejects from the center of the cavity. Utilizing jets equal in number to the acoustic mode number would cause each velocity vector emanating from the center to be accelerated. The flow field generated by two jets appears to conform more ideally to that of the second acoustic mode (fig. 2). Again, the speed of jet rotation must equal f_n/n. Modes of lower order than the number of jets cannot be generated if all jets are identical.

The pressure amplitude of a given mode would increase with an increase in total jet pressure and jet area. Increasing the total pressure increases both the jet flow rate and

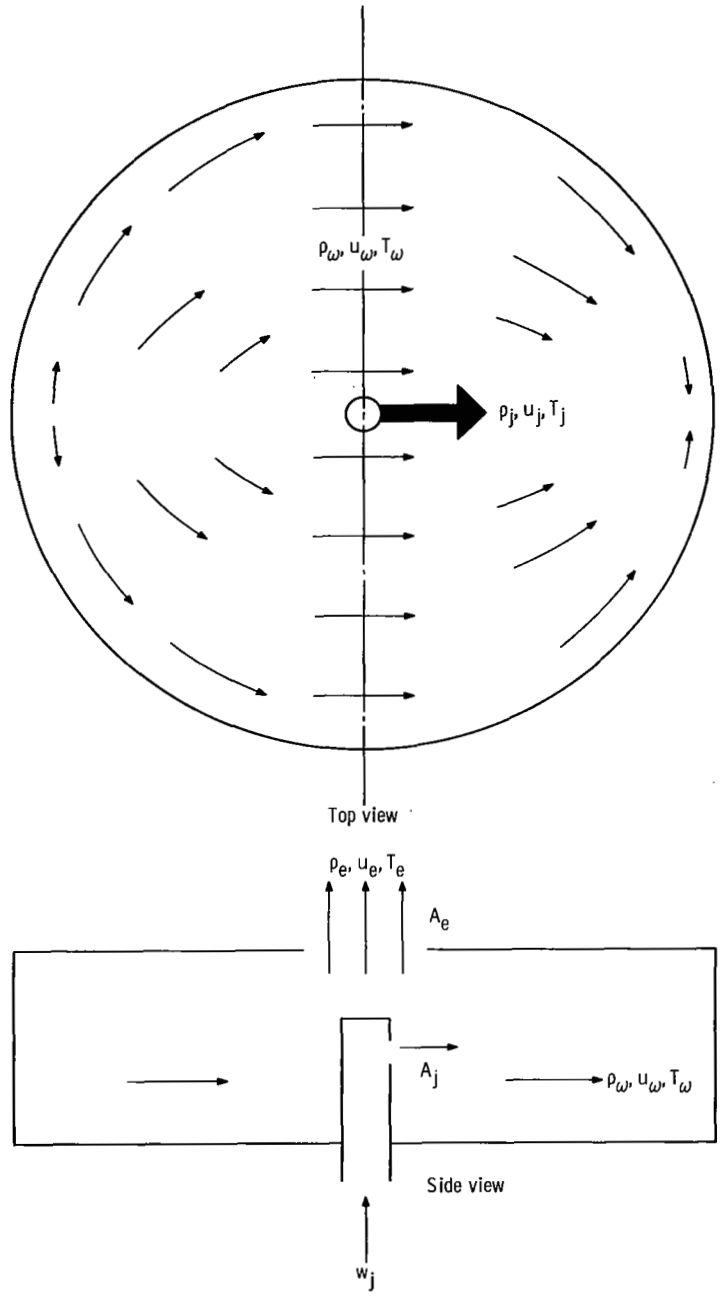

Figure 4. - Mass flow of acoustic wave, gas jet, and exhaust.

the pressure expansion ratio, thereby increasing the jet flow energy or jet power (see appendix B). An increase in jet area increases the jet power by virtue of the increase in mass flow rate. With critical jet flow, a divergent nozzle should also increase jet power because jet velocity is increased. If it is assumed that jet power is converted to acoustic power, any of these increases in jet power may be expected to give some increase in pressure amplitude. Pressure amplitudes, however, depend on the difference between losses and gains. These may vary nonlinearly with flow rate and amplitude and significantly effect the relation between pressure amplitude and jet power.

On the basis of reference 1, several characteristics should be exhibited when high amplitude pressure oscillations are generated. The wave shape should remain symmetrical with time about the peak pressure, and the wave should be free of any shocks. The frequency of the oscillations for any of the lower order resonant modes should decrease with an increase in amplitude.

GENERATOR CONFIGURATIONS

The acoustic generator used for the experimental investigation is shown schematically in figure 5, and an assembly view of the mechanical design is given in figure 6. The acoustic cavity is a short cylindrical section, 1.1 inches (2.8 cm) long, with provisions for using either an 8- or 12-inch (20.3 and 30.5 cm) diameter cylinder. A 1-inch (2.54 cm) diameter exhaust port at the center of the top plate was used to vent the cavity. The radially alined orifice at the center of the cavity is in a removable

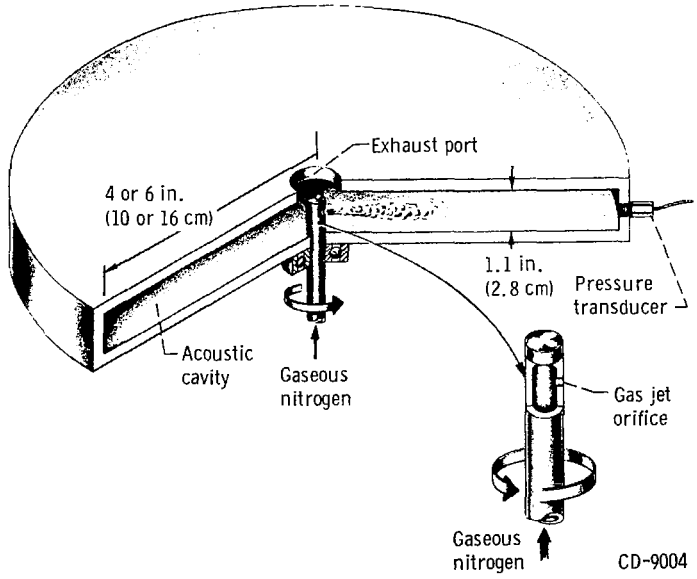

Figure 5. - Schematic of acoustic generator.

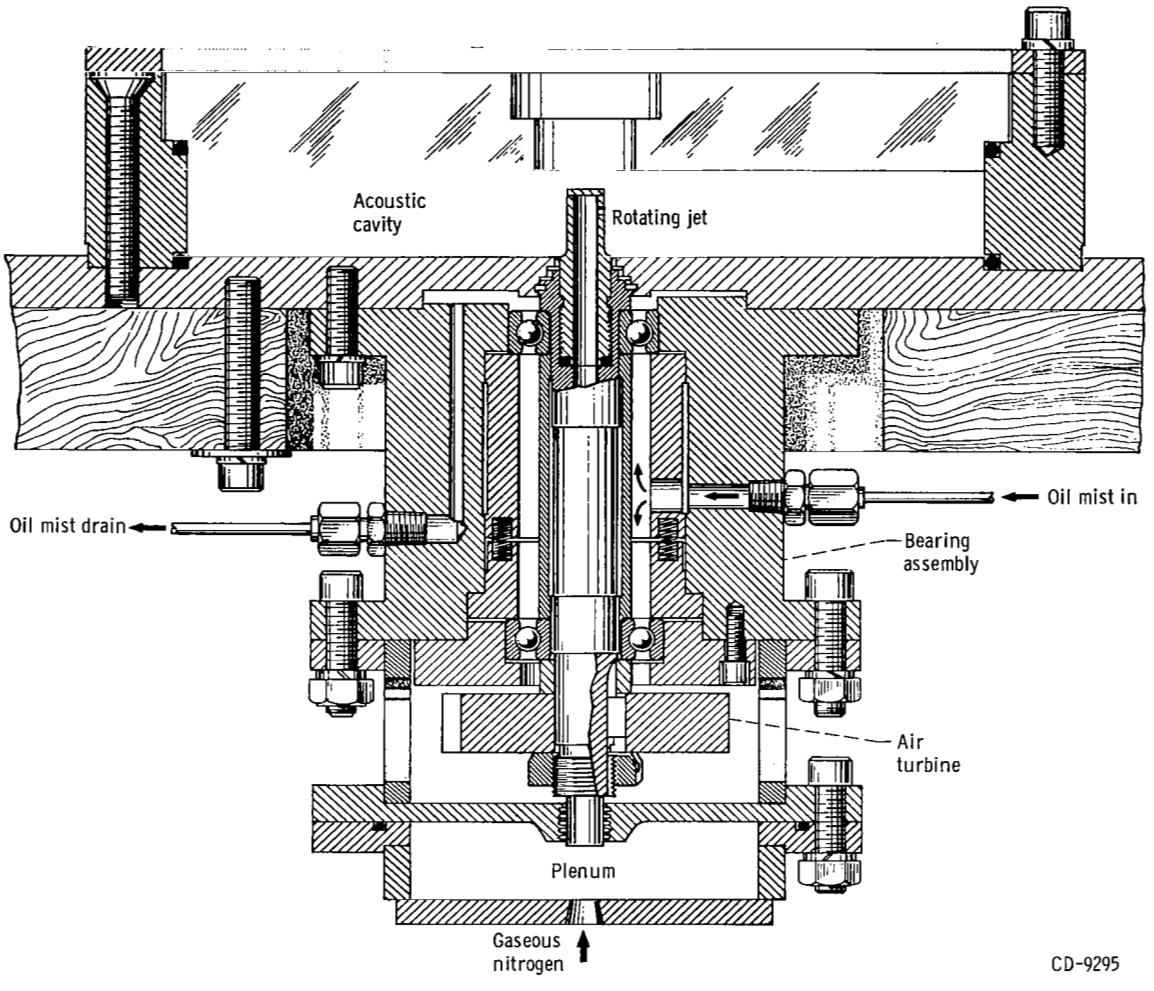

Figure 6. - Assembly view of acoustic generator.

extension of the hollow shaft. Gaseous nitrogen is fed to the orifice through the shaft from a plenum supplied by pressure regulated gas from a high pressure source of about 2000 psia (138×10^5 N/m^2). An air turbine between the plenum and bearing rotates the gas jet at speeds up to 70 000 rpm. A piezoelectric pressure transducer mounted flush with the cylindrical wall of the cavity was used to indicate pressure-time variations on a cathode-ray oscilloscope. Rotational speed was indicated on a digital counter from a signal supplied by a reluctance pickup mounted next to the turbine rotor. Mean cavity pressure was indicated with a bourdon element pressure gage.

Geometric changes of the radially alined orifice were accomplished by interchanging the extension of the hollow shaft. Orifice configurations are shown in figure 7. These include single orifices of 1/16, 3/32, 1/8, and 3/16-inch (0.159-, 0.238-, 0.318-, and 0.477 cm) diameter, diametrically opposed orifices of 3/32-inch (0.238-cm)

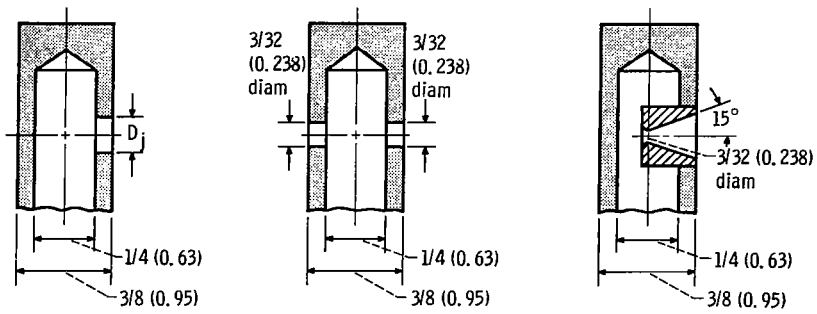

(a) Single orifice. Jet diameter, 1/16, 3/32, 1/8, and 3/16 inch (0.159, 0.238, 0.318, and 0.477 cm).

(b) Double orifice.

(c) Divergent nozzle.

Figure 7. - Jet configurations. All linear dimensions are in inches (cm).

diameter, and a divergent nozzle with a throat diameter of 3/32 inch (0.238 cm) and an area ratio of about 3 to 1.

EXPERIMENTAL PROCEDURE

The experimental evaluations were basically a parametric study about the single 3/32-inch (0.238 cm) diameter orifice in the 12-inch (30.5 cm) diameter cavity. Peak-to-peak pressure amplitudes in the cavity as a function of rotational speeds were measured for orifice supply pressures of 62.5, 125, 250, 500, and 1000 psia (4.3×10^5, 8.6×10^5, 17.2×10^5, 34.5×10^5, 69.0×10^5 N/m^2), for this 3/32-inch (0.238-cm) diameter orifice. Critical flow rates for these pressures are 0.01, 0.02, 0.04, 0.08, and 0.16 pound per second (4.5, 9, 18, 36, and 72 kg/sec), respectively. A more limited test of this orifice was made in the 8-inch (20.3-cm) diameter cavity. The other orifice configurations were also tested over a more limited range of flows in the 12-inch (30.5-cm) diameter cavity.

Peak-to-peak pressure amplitudes were determined from visual observations of oscilloscope deflections. A 150 to 20 000 hertz band pass filter was used for these measurements. Rotational speeds were selected and established to give well defined amplitude-speed response curves. Oscilloscope deflections of unfiltered signals were photographed at some conditions to record wave shapes.

Mean cavity pressure measurements during high amplitude resonance were unreliable. They were assumed to be the same as for nonresonant conditions and are shown as a function of flow rate in figure 8.

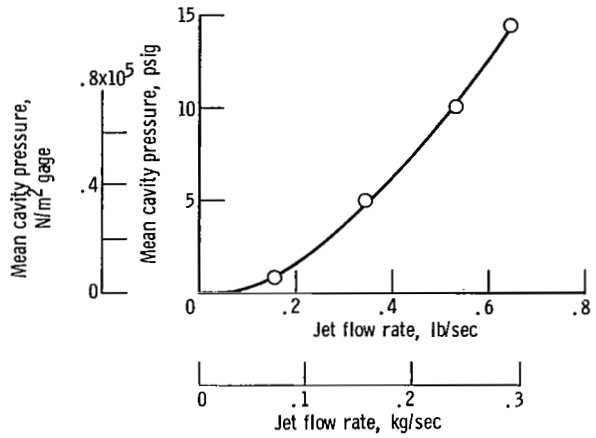

Figure 8. - Increase in cavity pressure with jet flow rate.

EXPERIMENTAL RESULTS AND DISCUSSION

The basic experimental result in this study is a response curve showing the peak-to-peak pressure amplitude at the circumference of the acoustic cavity as a function of the rotational speed of the gas jet. The effect of specific variables on this response curve are presented and discussed.

Jet Total Pressure

The response curves for the single 3/32-inch (0.238-cm) diameter orifice in the 12-inch (30.5-cm) diameter cavity are shown in figure 9. Three distinct resonant peaks are shown for each jet total pressure. The peaks at the highest rotational speeds are those of the first traveling transverse mode. The peaks at lower speeds exhibited frequencies that were 2 and 3 times the rotational speed and corresponded to the second and third traveling transverse modes, respectively. A single jet oriented with one of the velocity vectors emanating from the center was adequate to produce higher order acoustic modes of appreciable amplitude. At a jet total pressure of 1000 psia (69.0×10^5 N/m^2), peak-to-peak pressure amplitudes of 24, 12, and 6.5 psi (1.65×10^5, 0.83×10^5, and 0.45×10^5 N/m^2) were obtained for the first, second, and third modes, respectively. These amplitudes correspond to sound pressure levels of 189, 183, and 178 decibels and values of ϵ of 0.925, 0.554, and 0.346. The frequencies of these modes at their lowest measured amplitudes are 647, 1078, and 1485 hertz. From equation (6) these frequencies indicate speeds of sound of 1103, 1110, and 1112 feet per second (336.2,

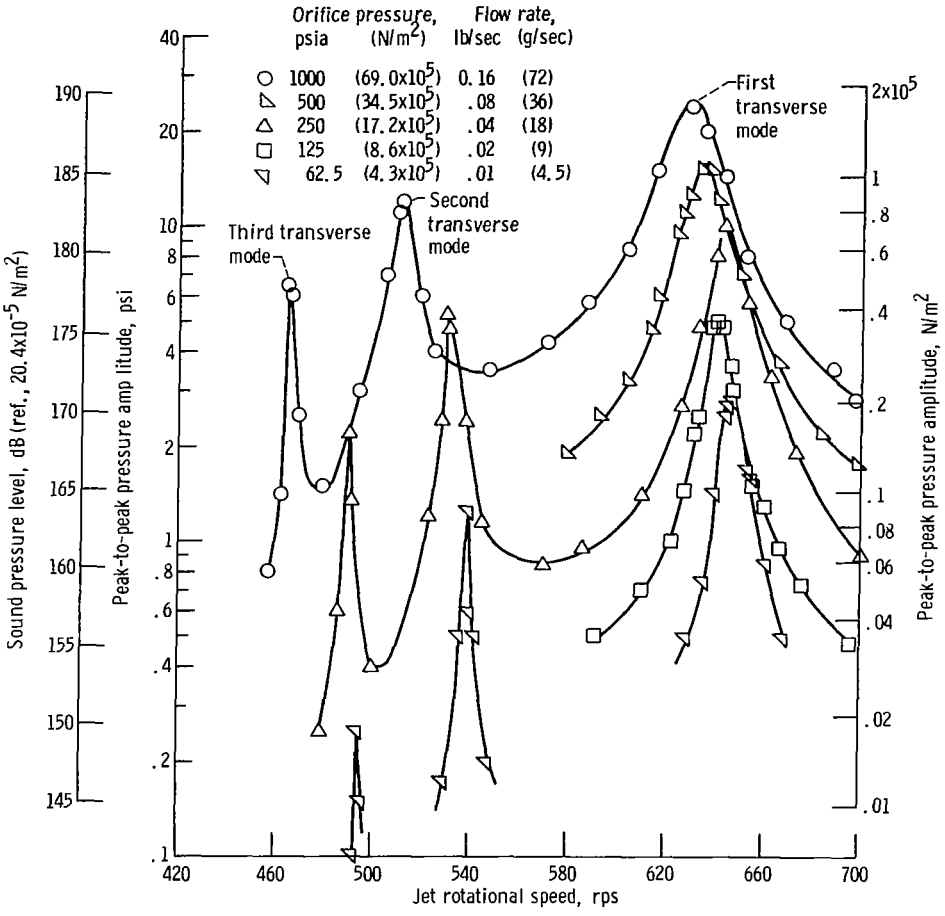

Figure 9. - Response of 3/32-inch (0.238-cm) diameter orifice in 12-inch (30.5-cm) diameter cavity.

338.3, and 338.6 m/sec) which correspond to temperatures of 490°, 492°, and 493° R (272°, 273°, and 273.5° K). These temperatures are suppressed by about 10° R (5.55° K) from the jet total temperature.

Increasing the jet total pressure increased the amplitude of all modes and generally decreased the resonant frequency as predicted in reference 1. Wave amplitude and sound pressure level as a function of jet total pressure are shown in figure 10. Amplitude appears proportional to jet total pressure at low values but becomes less than proportional with increasing jet pressure. An upper limit of amplitude with increasing jet pressure, however, has not been reached.

The effect of pressure amplitude on wave shape at the resonant peak of the first

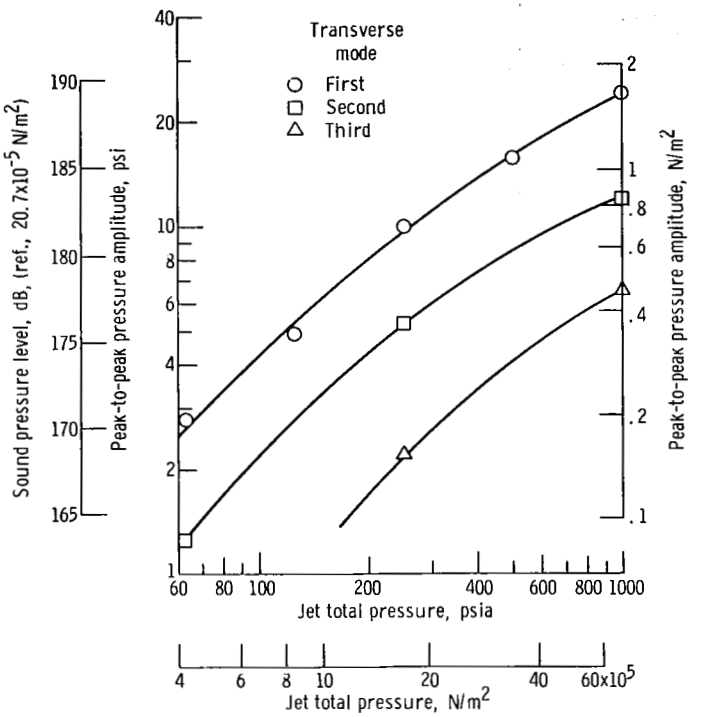

Figure 10. - Maximum resonant amplitudes with 3/32-inch (0.238-cm) diameter orifice in 12-inch (30.5-cm) diameter cavity.

mode is shown in figure 11(a). Nonlinearity increases with amplitude, but the wave shape remains symmetrical and free of shocks as indicated in figure 3 and reference 1. The change in wave shape with jet rotational speed at a jet total pressure of 250 psia (17.2×10^5 N/m^2) is shown in figure 11(b). As rotational speed is reduced, a frequency doubling is noted and successive higher mode resonant conditions are reached. Wave symmetry is lost at nonresonant conditions; however, the wave remains free of shocks.

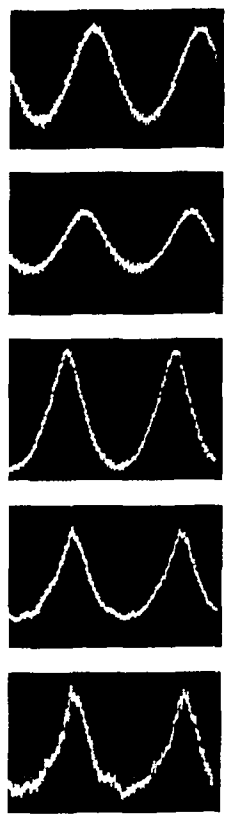

Peak to peak pressure amplitude, $(\Delta P)_{pp}$, psi	(N/m^2)	Frequency, f_n, Hz	Jet flow total pressure, P_j, psia	(N/m^2)
2.8	(0.19×10^5)	647	62.5	(4.3×10^5)
5.0	(0.35×10^5)	641	125	(8.6×10^5)
10.0	(0.69×10^5)	644	250	(17.2×10^5)
15.5	(1.07×10^5)	634	500	(34.5×10^5)
24.0	(1.65×10^5)	629	1000	(69.0×10^5)

(a) Resonant peaks of first transverse mode; unfiltered signals.

Figure 11. - Pressure - time wave shapes.

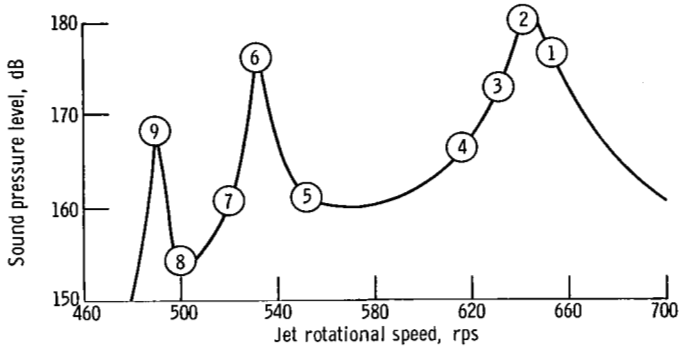

(b) Effect of rotational speed on wave shape for jet total pressure of 250 psia (17.2x10^5 N/m^2); 150- to 3000-hertz filtered signals.

Figure 11. - Concluded.

Orifice Diameter

First transverse mode resonance for a 3/16-inch (0.477-cm) diameter orifice is shown in figure 12 for the same jet total pressures as for the 3/32-inch (0.238-cm) diameter orifice presented in figure 10. Peak-to-peak pressure amplitudes are in all cases higher for the large orifice. At a total pressure of 1000 psi (69.0×10^5 N/m^2), the amplitude is 38 psi (2.62×10^5 N/m^2) compared with 24 psi (1.65×10^5 N/m^2) for the 3/32-inch (0.238-cm) diameter orifice. This corresponds to a sound pressure level of 193 decibels which is considerably higher than that obtained with high intensity drivers in reference 3. The wave shape at 193 decibels is also shown in figure 12.

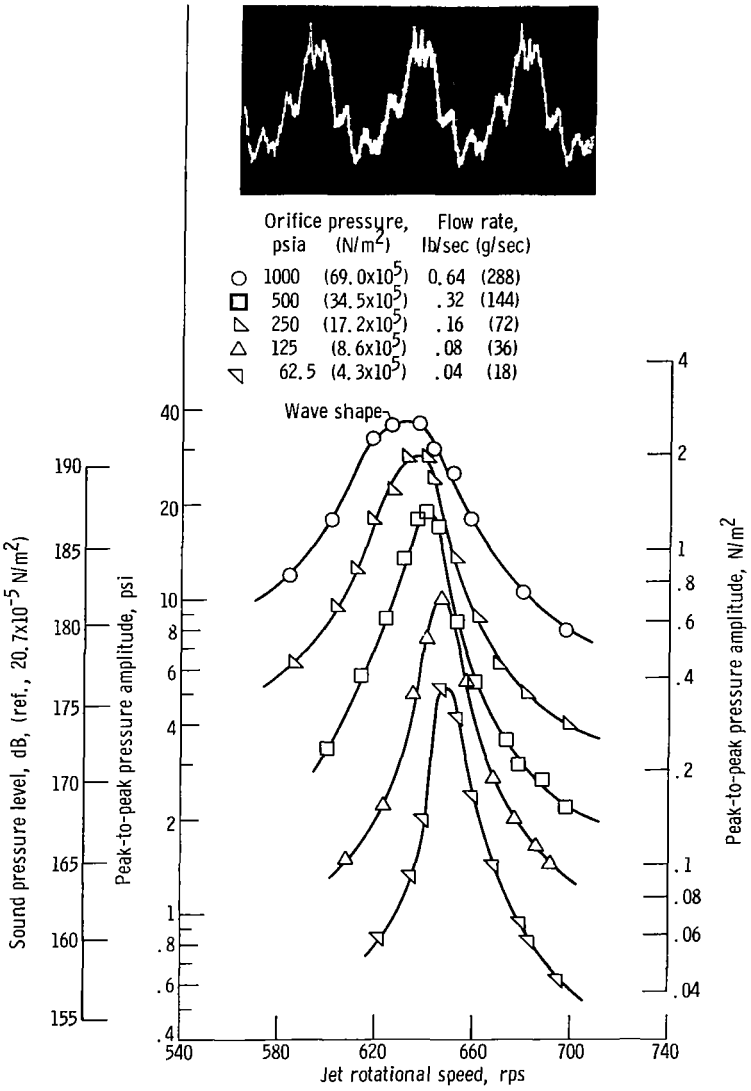

Figure 12. - Effect of orifice pressure and flow rate on response for 3/16-inch (0.477-cm) diameter orifice.

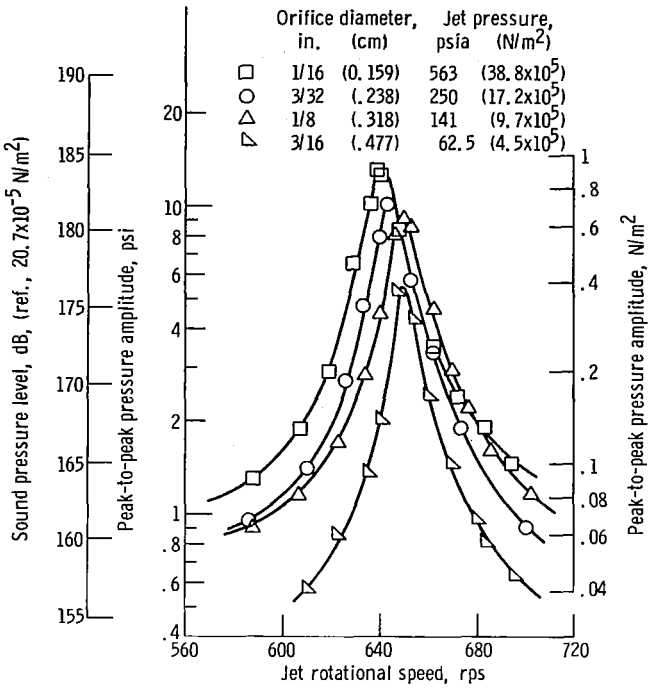

Figure 13. - Effect of orifice diameter on response of constant jet flow rate of 0.04 pound per second (18 g/sec).

Harmonic content of the wave appears appreciable, however, symmetry and shock-free conditions seem to prevail. Mean cavity pressure at this high amplitude condition is approximately 29 psia (1068 N/m^2) (fig. 8), whereas it was very nearly equal to 1 atmosphere (1×10^5 N/m^2) for most of the experiments performed in this study.

The effect of orifice diameter is also shown in figure 13. The response curves for orifice sizes of 1/16, 3/32, 1/8, and 3/16 inch (0.159, 0.238, 0.318, and 0.477 cm) in diameter are shown for total jet pressures which would give identical jet flow rates. The peak resonant amplitude increases with a decrease in orifice size. Jet total pressure, however, is high for the small orifice, and the higher jet power may account for the increase in amplitude.

Divergent Nozzle

The response curves at several jet total pressures for jet flow from a divergent nozzle is shown in figure 14. The amplitudes at the resonant peaks are comparable to

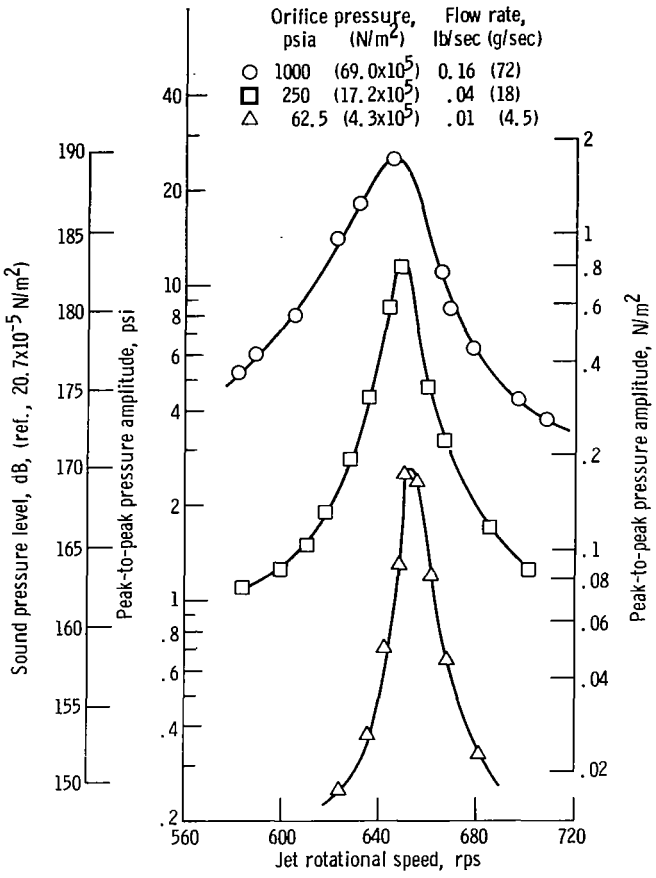

Figure 14. - Response of 3 to 1 area ratio nozzle; fundamental mode in 12-inch (30.5-cm) diameter cavity.

that for an orifice of equal minimum area. This result may not be general because a precision and polished nozzle was not used; therefore, the nozzle flow process may have been less than ideal.

Multiple Jets

The response curves for two radial jets in diametrically opposite directions are shown in figure 15. The resonant condition shown is the second transverse mode. Resonance did not occur at the first and third transverse mode frequencies. Pressure amplitude was 15 psi (1.03×10^5 N/m^2) compared with 12 psi (0.83×10^5 N/m^2) for a single orifice at a jet pressure of 1000 psia (69.0×10^5 N/m^2). This increase must be partially attributed to the higher jet flow rate for two jets compared with a single jet. The amplitude for the second mode with two jets, however, is significantly less than that of the first mode with a single jet.

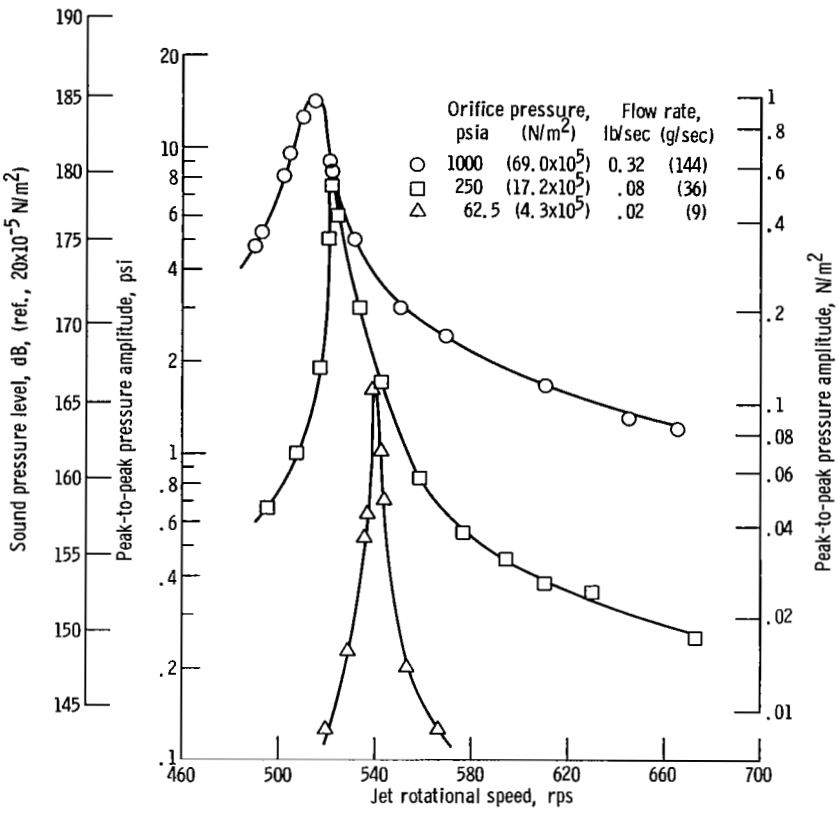

Figure 15. - Response for two opposed orifices of 3/32-inch (0.238-cm) diameter.

Cavity Diameter

First transverse mode resonance in an 8-inch (20.3-cm) diameter cavity using a single 3/32-inch (0.238-cm) diameter orifice is shown in figure 16. The theoretical resonant frequency for this cavity is 971 hertz for a speed of sound of 1110 feet per second (338.3 m/sec). At low jet total pressure, this frequency is approached, although there is a considerable decrease in frequency with increasing amplitude. Peak amplitudes are lower than obtained with a 12-inch (30.5 cm) diameter cavity at jet total pressures of 1000 and 250 psig (69.0×10^5 and 17.2×10^5 N/m^2), but the amplitude is higher at a pressure of 62.5 psig (4.3×10^5 N/m^2). Some erratic behavior was observed with this smaller cavity. At high values of jet total pressure and near resonance, the amplitude of the pressure oscillations fluctuated periodically. Confining the jet flow in the smaller cavity could have caused the unstable secondary effects (streaming flow, temperature changes, etc.) which interfered with the resonant conditions.

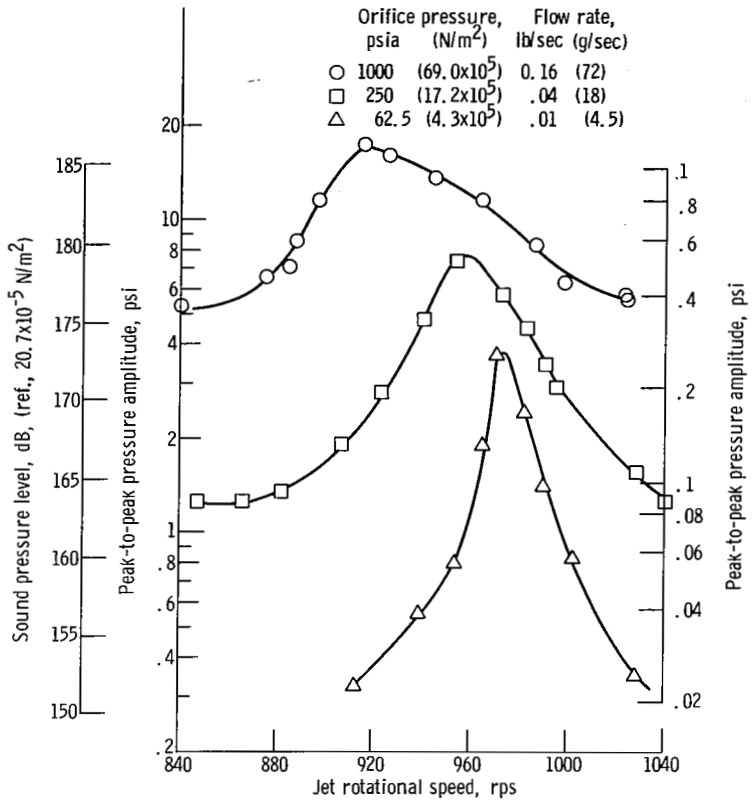

Figure 16. - Response of 3/32-inch (0.238-cm) diameter jet in 8-inch (20.3-cm) diameter cavity for first transverse mode.

Evidence of wheel flow or some other accumulation effect was pronounced for the higher modes in this 8-inch (20.3-cm) diameter cavity where two distinct and reproducible resonant curves were observed. Approaching cavity resonance by an increase in jet rotational speed produced one curve, whereas a decrease in speed produced the other. The frequency at peak amplitude differed for these two curves. Solid body rotation of the cavity gases caused by the streaming effect discussed in reference 1 could account for this difference if the magnitude of solid body rotation depended on the method used to approach resonance. Reference 1 implies that the magnitude of solid body rotation is not as strongly prescribed for higher modes as for the first mode. The occurrence of dual resonant peaks was not restricted to the 8-inch (20.3-cm) diameter cavity. Under some flow conditions, a less pronounced effect was observed for the higher modes in the 12-inch (30.5-cm) diameter cavity.

PERFORMANCE EVALUATION

The equilibrium pressure amplitude developed by an acoustic generator in a cavity is not in itself a measure of its performance efficiency; the equilibrium amplitude only reflects the condition where acoustic power generated is equal to the acoustic power lost. Performance is more accurately specified by the conversion efficiency of input power to acoustic power developed in appendix B. The efficiency is defined as the ratio of acoustic power developed by the rotating jet W_ω to the theoretical jet power $(W_j)_{th}$ given by frictionless adiabatic expansion of total jet pressure to mean cavity pressure. The expression for conversion efficiency given in appendix B is

$$\eta = \frac{W_\omega}{(W_j)_{th}} = \frac{2kE_\omega}{(W_j)_{th}} = \frac{2\pi(\Delta f)_{0.707} C_n V (\Delta P)_{pp}^2}{8\gamma W_j \frac{R}{m} T_j \bar{P} \frac{\gamma}{\gamma - 1} \left[1 - \left(\frac{\bar{P}}{P_j} \right)^{\frac{\gamma - 1}{\gamma}} \right]} \tag{7}$$

where C_n is equal to 0.861, 0.686, and 0.610 for first, second, and third transverse traveling modes, respectively.

Power required to rotate the jet has not been included in this efficiency expression. It is considered small although unknown. However, for a fixed air-turbine flow setting, the differences in rotational speed with and without jet flow were small, which indicated a small expenditure of shaft power due to jet flow. Regardless, equation (7) expresses the efficiency of the process rather than that of the overall generator.

The conversion efficiency given by equation (7) is expressed by the three parameters: acoustic energy E_ω damping coefficient k, and theoretical jet power $(W_j)_{th}$. These three parameters were computed for the resonant peaks for each of the generator configurations tested to obtain the conversion effiency for each configuration.

Acoustic Energy

Acoustic energy per unit weight of cavity gases $E_\omega / \bar{\rho} V$ is shown in figure 17. The energy increased with jet total pressure for all configurations except for the 3/16-inch (0.477-cm) diameter orifice at a high total pressure. Although the pressure amplitude with this orifice had the maximum observed value for all configurations, acoustic energy was not a maximum because of the high value of mean cavity pressure. In general, how-

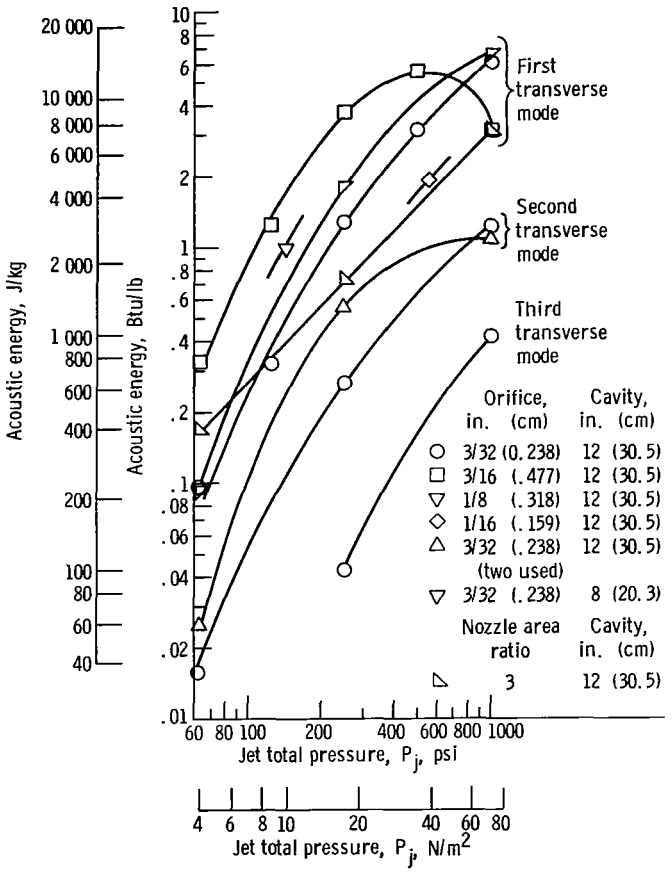

Figure 17. - Effect of generator parameters on acoustic energy content in resonant modes.

ever, acoustic energy increased with parameters which increased jet power, that is, with jet pressure, orifice diameter, and nozzle area ratio. Acoustic energy content of the cavity gases is lower for the small cavity and for the higher modes. The maximum energy content for all conditions is shown to be about 6 Btu per pound. Viscous dissipation of this energy would cause a temperature rise of 24° R indicating that the equivalent heat content of the acoustic energy is relatively high.

Damping Coefficient

The damping coefficients evaluated from the half-power band width of the resonant peaks are shown in figure 18. Acoustic damping, indicated by the value of the coefficient, may be expected to vary with the pressure amplitude, oscillatory frequency, chamber geometry, exhaust flow processes, and the turbulence or nonacoustic flow caused by jet expansion and mixing. Figure 18 shows an increase in the damping coefficient with jet total pressure for all generator configurations. This increase is probably caused by the increase in pressure amplitude and jet turbulences which accompanied an increase

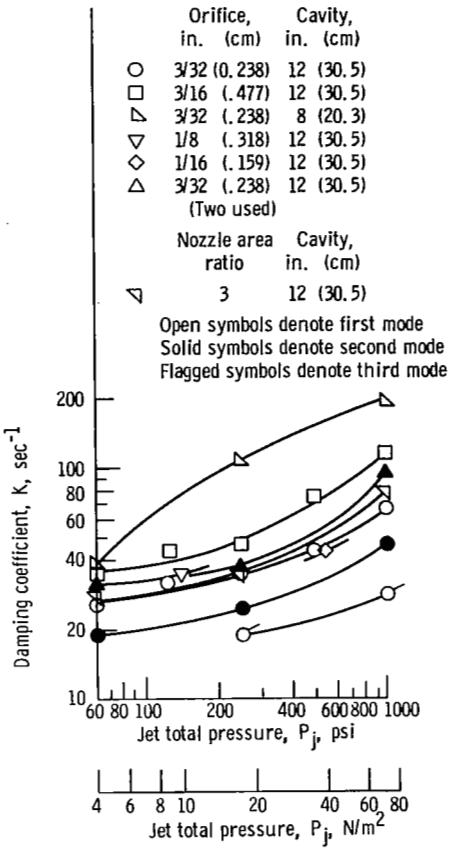

Figure 18. - Effect of generator parameters on temporal damping constant.

in total pressure. Amplitude and turbulence increases may also account for the small increase in damping with jet orifice size at a constant total jet pressure. As shown in figure 18, the damping increased with an increase in mode number for the same jet pressure. When compared on the basis of equal pressure amplitudes, however, the coefficients are nearly equal for all modes. The large values for the 8-inch (20.3-cm) diameter cavity are more difficult to interpret. Decreasing the size of the cavity increased the surface to volume ratio, increased the area of the exhaust port relative to the cavity area and probably increased the turbulent nature of the cavity gases for a given flow input. All these factors could contribute to an increase in the damping coefficient for the 8-inch (20.3-cm) diameter cavity. Increasing the oscillatory frequency by decreasing the cavity size or by exciting higher order modes in the 12-inch (30.5-cm) diameter cavity appeared to have a small effect on the damping coefficient. Extracting the magnitude of the frequency effect on damping from these results, however, depends on knowing the functional relation of the other dependent variables.

The curves shown in figure 18 appear to have an asymmetric value at low total jet pressures. An asymptotic value of 10 to 20 reciprocal seconds is obtained from an extrapolation with respect to pressure amplitude. Damping coefficients of this magnitude are consistent with those indicated in references 2 and 5 for conditions of no flow and small pressure perturbations.

Acoustic Power

The increase in acoustic power, W_ω, with theoretical jet power $(W_j)_{th}$ is shown in figure 19. Jet power varied from 500 to 50 000 watts for these tests. A maximum acoustic power of 10 000 watts was realized in the first transverse mode with the 3/16-inch (0.238-cm) diameter orifice. Acoustic power was nearly an order of magnitude lower for each increase in mode number at the same value of jet power. Acoustic power did not vary directly with jet power. Rather, acoustic power more nearly varied with jet power by the relation

$$W_\omega \sim (W_j)_{th}^{1.6}$$

Conversion Efficiency

Conversion efficiency of jet power to acoustic power is the ratio of the quantities displayed in figure 19. These efficiencies are shown in figure 20 against jet total pressure. In general, efficiency increases with an increase in jet total pressure and is almost an order of magnitude lower for each increase in acoustic mode number. Maximum efficiency was obtained with the divergent nozzle giving a value of 44 percent at a total pressure of 1000 psig (69.0×10^5 N/m^2). This particular divergent nozzle, however, was only marginally better than a simple orifice of the same size. The effect of orifice size is indefinite in this comparison; however, the 3/16-inch (0.477-cm) orifice attained an optimum value of 28 percent at a jet pressure of about 600 psia (40×10^5 N/m^2). If there are optimum values, the other curves imply that they would occur at jet pressures above 1000 psia (69.0×10^5 N/m^2).

Using two jets to generate the second transverse mode gave about a 25 percent increase in efficiency over that for a single jet. The efficiency, however, remains low and does not approach the values for the first mode at comparable jet flow rates.

The effect of orifice diameter on efficiency for a constant jet flow rate is shown in figure 21. Efficiency increases with a decrease in jet size. Jet total pressure is high

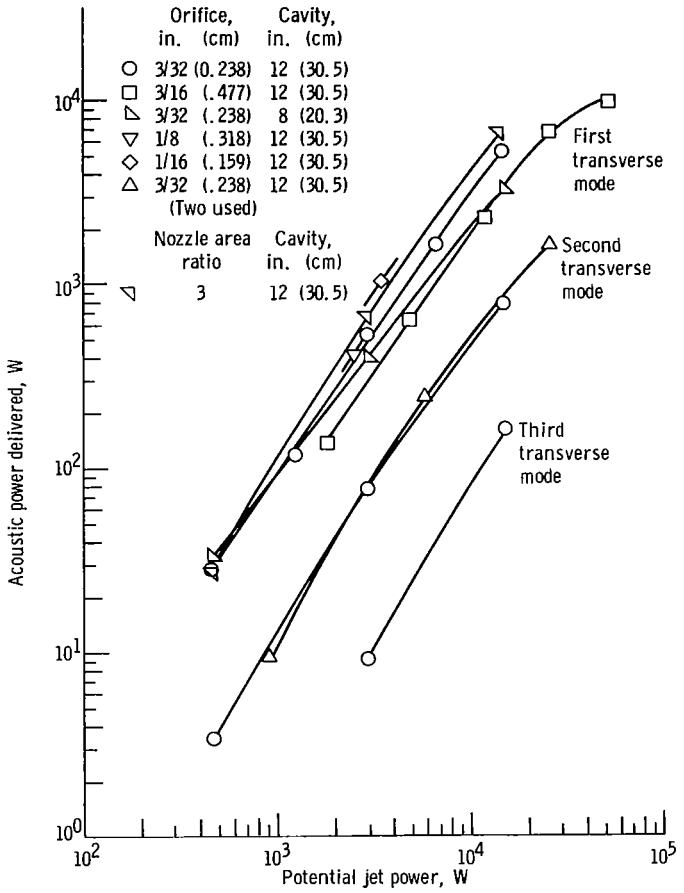

Figure 19. - Effect of generator parameters on delivered acoustic power.

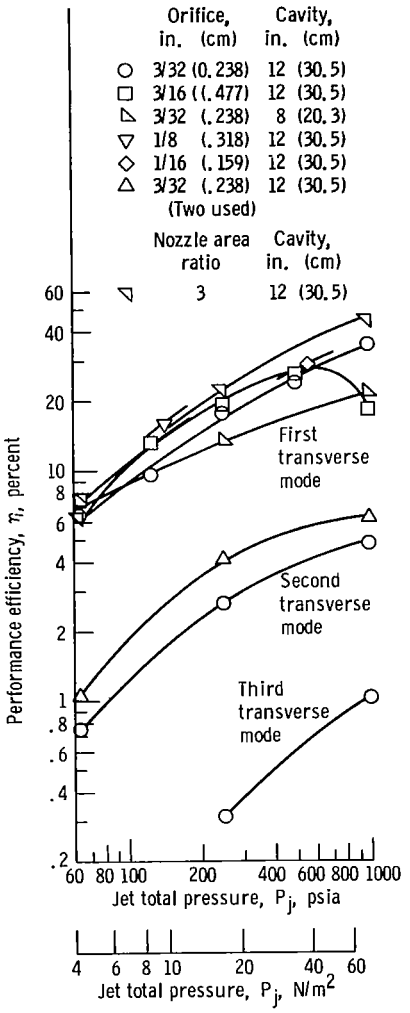

Figure 20. - Effect of generator parameters on performance efficiency.

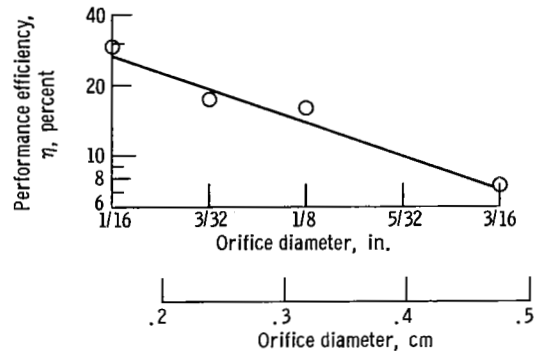

Figure 21. - Effect of orifice diameter on performance at constant flow rate.

for small jets, and this confirms the general behavior exhibited in figure 20 where efficiency increased with an increase in jet pressure.

The conclusion reached from this study of generator configurations is that high jet total pressures generally give high efficiencies. The jet expansion and mixing process that accompanies a high pressure jet appears to be favorable in amplifying the mass flow associated with the acoustic modes. Increasing the jet pressure, however, increases the jet penetration and produces a more turbulent mixing and expansion process. Because of such turbulent losses, an optimum pressure for conversion efficiency, as observed with the 3/16-inch (0.477-cm) diameter orifice, may occur. Confining a given jet flow in a smaller cavity would also increase the turbulent nature of the mixing process. The decrease in efficiency with the 8-inch (20.3-cm) diameter cavity (fig. 20) is attributed to this effect. A less ideal mixing process is also visualized for the higher resonant modes than for the first mode with the same jet flow conditions. These observations imply that an optimum jet flow and mixing process exists for each cavity configuration and mode of oscillation. The combined functional effect of configurations and test conditions to give optimum efficiencies cannot be specified from the limited range of variables investigated in this study.

CONCLUDING REMARKS

The method of analysis used in this study to compute the generator efficiency must be taken as a first-order approximation of the performance. Although acoustic properties within the cavity were expressed by first-order terms for ideal waves, higher order terms and a survey of the wave patterns within the cavity are needed to accurately evaluate the strong waves observed in this study. The results of the analysis, however, are not considered to be substantially in error. An evaluation of the rms pressure for the actual wave shapes agreed to within 10 percent with that of a sine wave of the same peak-

to-peak amplitude. The energy content of the wave from first-order terms, therefore, is not appreciably in error. The method of analysis and the numerical procedures involved in a more accurate performance analysis remain to be developed.

The principle demonstrated in this study is not limited to the injection of an inert gas. A combustion process could be used to supplant the pressurized gas system. Ideally, the velocity vector through the center of the cavity for the first mode suggests that a small rotating duct burner operated on a ramjet principle could be used to increase the mass flow associated with the acoustic mode and thus amplify or drive the mode.

An interesting deviation is the frequently used surface wave analogy for acoustic oscillations. A rotating water jet at the center of a circular basin should develop strong traveling surface waves.

SUMMARY OF RESULTS

An experimental study on the generation of strong traveling transverse acoustic modes with a rotating gas jet gave the following effects of configuration and operating condition changes on performance:

1. A single rotating jet generated the first and higher order acoustic modes depending on rotational speed. The first mode occurred when rotational speed corresponded to the frequency of the acoustic mode. Higher modes occurred at lower speeds where more than one pressure oscillation was obtained for each rotation of the jet. Acoustic modes were generated when the rotational speed was equal to the resonant frequency divided by the mode number.

2. The pressure amplitude of an acoustic mode generally increased with an increase in jet total pressure. The conversion efficiency of jet power to acoustic power also increased with an increase in jet total pressure; however, an optimum condition can occur beyond which efficiency decreases.

3. The pressure amplitude of an acoustic mode and the efficiency decreased with an increase in jet orifice diameter at a constant jet flow rate. Pressure amplitude also decreased with an increase in diameter at constant jet total pressure; however, the effect on efficiency was indefinite.

4. Jet flow from a divergent nozzle gave pressure amplitudes comparable to that of an orifice, and a marginal increase in conversion efficiency.

5. A decrease in the acoustic cavity diameter for identical jet flow conditions generally reduced the strength of the mode and the conversion efficiency. Other results imply that this is not a general behavior. It may be possible to optimize jet flow conditions for specific cavity dimensions.

6. Generating the second transverse mode with two radial jets in diametrically

opposite directions increased the strength of the mode and conversion efficiency over that for a single jet of the same size and total pressure.

7. A 3-16-inch (0.477-cm) diameter jet at a total pressure of 1000 psia (69.0×10^5 N/m^2) developed peak-to-peak pressure amplitudes of 38 psi (2.62×10^5 N/m^2) at the circumference of a 12-inch (30.5-cm) diameter cavity for the first transverse mode frequency of 635 hertz. The computed acoustic power delivered was 10 000 watts while the potential jet power was 50 000 watts. A maximum conversion efficiency of 44 percent was obtained with a divergent nozzle with a 3/32-inch (0.238 cm) diameter throat. For fixed jet flow rates, the peak-to-peak pressure amplitudes were lower for the higher order transverse modes and conversion efficiencies decreased nearly an order of magnitude for each increase in mode number.

Lewis Research Center,
National Aeronautics and Space Administration,
Cleveland, Ohio, August 22, 1967,
128-31-06-02-22.

APPENDIX A

SYMBOLS

A	area, m^2
a	speed of sound, ft/sec; m/sec
B	dimensionless constant
C_v	specific heat at constant volume, J/(kg)(^oK)
E	energy, J
$\mathcal{E}$	energy associated with conduction and viscous effects, J/kg
f	frequency, Hz
$(\Delta f)_{0.707}$	band width frequency at half-power, Hz
i	index
$J_n(\alpha)$	Bessel function of the first kind of order n
k	damping coefficient
M	apparent Mach number of acoustic wave
m	molecular weight, kg/mole
n	acoustic mode number of traveling wave
P	total pressure, psia; N/m^2
$(\Delta P)_{pp}$	peak-to-peak pressure amplitude, psi; J/kg
p	free stream pressure, psia; N/m^2
R	radius of coustic cavity, m
r	radial position, m
$\mathcal{R}$	gas constant, J/(^oK)(mole)
T	free stream temperature, ^oK
t	time, sec
u	velocity, m/sec
V	volume of acoustic cavity, m^3
W	power, W
w	mass flow rate, kg/sec
z	axial length of acoustic cavity, m
α	nondimensional radial coordinate $\omega r/a_o$
γ	ratio of specific heats
ϵ	amplitude parameter
ρ	gas density, kg/m^3
η	conversion efficiency
ω	frequency, rad/sec
θ	angle in cylindrical coordinator, rad

Subscripts:

e	exhaust flow
j	jet flow
n	conditions for acoustic mode of order n
o	initial condition
th	theoretical
α	radial position
ω	conditions associated with acoustic wave
r	radial component
θ	angular component

APPENDIX B

PERFORMANCE ANALYSIS

The flow process of interest in this study is the interaction of the rotary gas jet with the gas flow associated with the acoustic mode. Jet gases represent energy which can be transferred to the acoustic mode. The efficiency of this energy transfer process is one measure of the acoustic generator performance. Developed in this appendix is an analytical expression for the conversion efficiency of jet flow energy or jet power to acoustic power.

A definition of the conversion efficiency is obtained from a consideration of an energy balance for the acoustic generator. The total energy within the acoustic cavity is the sum of an acoustic energy and a steady energy based, respectively, on perturbed and mean values of gas properties. The rate of change of this total energy depends on the difference between the energy gained and lost. Such gains and losses are primarily described by ideal jet expansion and exhaust flow processes; however, these must be modified by viscous and conduction effects occurring within the cavity. Emphasizing the flow processes and lumping the viscous and conduction factors associated with gains and losses yields the energy balance equation

$$\frac{d}{dt}\int^{V} \bar{\rho}\left(\frac{\vec{\bar{u}}^2}{2} + C_v\bar{T}\right)dV + \frac{d}{dt}\int^{V}\left[\frac{\rho\vec{u}^2 - \bar{\rho}\vec{\bar{u}}^2}{2} + C_v(\rho T - \bar{\rho}\bar{T})\right]dV$$

$$= w_j\left[\frac{u_j^2}{2} + \frac{1}{J}\int_{p_j}^{\bar{P}} \frac{1}{\rho}\,dp + \mathcal{E}_j\right] - w_e\left[\frac{u_e^2}{2} + \frac{1}{J}\int_{\bar{P}}^{p_e} \frac{1}{\rho}\,dp + \mathcal{E}_\omega\right] \qquad \text{(B1)}$$

The term $\mathcal{E}_j$ accounts for the irreversibility of the jet expansion and mixing processes. Viscous dissipation and conduction effects associated with the acoustic mode and exhaust flow are represented by $\mathcal{E}_\omega$.

Equation (B1) is an integrated form of the energy equation which gives the net change of energy in the acoustic cavity in terms of steady flow quantities. It is valid even though the rotary jet causes little or no acoustic resonance. In the event that no oscillations occur, the jet flow only affects the mean properties of the cavity gases. Assuming the mean value of these properties are unaffected when resonance occurs, for instance,

nonvarying for any fixed jet flow rate, equation (B1) defines an acoustic energy balance. It essentially states that the rate of change of acoustic energy within the cavity is equal to the difference between jet power converted to acoustic form and the acoustic power lost by exhaust flow and viscous damping.

The pressure amplitudes reported in this study are at equilibrium conditions where there is no rate of change of acoustic energy in the cavity. For such conditions, equation (B1) shows that jet power is converted to acoustic power in amounts equal to the acoustic losses. A measure of the acoustic losses, therefore, is equivalent to measuring the acoustic power delivered by the jet flow. The losses can be evaluated from the experimental results.

A second order differential equation is usually adequate to represent forced ocsillations in acoustic resonators with damping (ref. 4). For such resonators, the magnitude of the acoustic losses are indicated by a coefficient of damping K such that the fractional rate of change of acoustic energy due to losses alone is given by

$$\frac{dE_\omega/E_\omega}{dt} = -2K \tag{B2}$$

Assuming such representation for the acoustic generator used in this study, the acoustic power lost and, at equilibrium, the acoustic power delivered by the jet is given by

$$W_\omega = 2KE_\omega \tag{B3}$$

or

$$w_j\left[\frac{u_j^2}{2} + \frac{1}{J}\int_{p_j}^{\bar{P}} \frac{1}{\rho}\,dp + \mathcal{E}_j\right] = 2k\int^{V}\left[\frac{\rho\vec{u}^2 - \bar{\rho}\vec{\bar{u}}^2}{2} + C_v(\rho T - \bar{\rho}\bar{T})\right]dV \tag{B4}$$

In a real system, the left side of equation (B4) represents a less than ideal jet expansion and mixing process. The acoustic power delivered by the jet, therefore, is some fraction of that potentially available. A measure of the conversion efficiency of jet power to acoustic power is the ratio of the actual acoustic power delivered to that potentially or theoretically available.

$$\eta = \frac{W_\omega}{(W_j)_{th}} \tag{B5}$$

Theoretical jet power is defined as the value of the left side of equation (B4) for fractionless adiabatic expansion of an ideal gas for the total available pressure ratio.

$$(W_j)_{th} = w_j R \frac{T_j}{m} \frac{\gamma}{\gamma - 1} \left[1 - \left(\frac{\bar{P}}{P_j} \right)^{(\gamma-1)/\gamma} \right] \tag{B6}$$

Using the foregoing relations, the expression for conversion efficiency is

$$\eta = \frac{2k \int^{V} \left[\frac{\rho \vec{u}^2 - \bar{\rho} \vec{u}^2}{2} + C_v(\rho T - \bar{\rho}\bar{T}) \right] dV}{w_j R \frac{T_j}{m} \frac{\gamma}{\gamma - 1} \left[1 - \left(\frac{\bar{P}}{P_j} \right)^{(\gamma-1)/\gamma} \right]} \tag{B7}$$

Equation (B4) was evaluated for all conditions of peak resonance observed experimentally. As in reference 5, the coefficient of damping was obtained from the frequency difference at the half-power pressure amplitudes of the response curves where

$$k = \pi(\Delta f)_{0.707} \tag{B8}$$

Mean velocities associated with flow through the cavity and other sources were neglected in evaluating the integral for acoustic energy in the cavity. In evaluating this integral, it was expressed as

$$E_\omega = \int_0^R \int_0^1 \int_0^{2\pi} \left[\frac{\rho \vec{u}^2}{2} + C_v(\rho T - \bar{\rho}\bar{T}) \right] r \, dr \, dz \, d\theta \tag{B9}$$

Equation (B9) was evaluated for constant values of r which represented the mean radii of equal concentric areas of the circular cross section and a mean energy per unit volume was established. Acoustic energy was obtained from the relation

$$E_\omega = V \frac{\sum^{i} (E_\omega)_\alpha}{i} \tag{B10}$$

where

$$(E_\omega)_\alpha = \overline{2\pi} \int_0^{2\pi} \left[\frac{\rho \vec{u}^2}{2} + C_v(\rho T - \overline{\rho T}) \right] d\theta \tag{B11}$$

The expressions for ρ, T, u_θ, and u_r at t = 0 from equations (1) to (5) were used. The velocity $\vec{u}$ was obtained from the vector sum of u_θ and u_r, giving

$$\vec{u}^2 = \epsilon^2 a_0^2 \left\{ \left[n \frac{J_n(\alpha)}{\alpha} \right]^2 + \left[J_{n-1}^2(\alpha) - 2nJ_{n-1}(\alpha) \frac{J_n(\alpha)}{\alpha} \right] \sin^2 n\theta \right\} \tag{B12}$$

Substituting yields for equation (B11)

$$(E_\omega)_\alpha = \overline{2\pi} \int_0^{2\pi} \frac{\epsilon^2 a_0^2 \overline{\rho}}{2} \left\{ \left(1 + \epsilon J_n(\alpha) \cos n\theta\right) \left[\frac{nJ_n(\alpha)}{\alpha} \right]^2 + \left[J_{n-1}^2(\alpha) - 2nJ_{n-1}(\alpha) \frac{J_n(\alpha)}{\alpha} \right] \times \sin^2 n\theta \right\} d\theta + C_v \overline{\rho T} \left[\gamma \epsilon J_n(\alpha) \cos n\theta + (\gamma - 1)\epsilon^2 J_n^2(\alpha) \cos^2 n\theta \right] d\theta \tag{B13}$$

Integrating (B13) gives

$$(E_w)_\alpha = \frac{(\Delta P)_{pp}^2}{8\gamma \overline{P}} \left[\left(\frac{J_n(\alpha)}{J_n\left(\frac{\omega}{a_0}\right)} \right)^2 \left\{ \left(\frac{n}{\alpha} \right)^2 + \frac{1}{2} \left[\left(\frac{J_{n-1}(\alpha)}{J_n(\alpha)} \right)^2 - 2 \left(\frac{n}{\alpha} \right) \left(\frac{J_{n-1}(\alpha)}{J_n(\alpha)} \right) \right] + \frac{1}{\gamma} \right\} \right] \tag{B14}$$

where

$$\rho a_0^2 = \overline{P}\gamma \quad C_v \overline{\rho}\, \overline{T} = \frac{\overline{P}}{(\gamma - 1)}$$

and

$$\epsilon = \frac{(\Delta P)_{pp}}{2\gamma \overline{P} J_n\left(\frac{\omega}{a_0}\right)}$$

have been used. Evaluating (B14) for r/R of 0.935, 0.790, 0.612, and 0.352 for the first three traveling transverse modes gives

$$E_\omega = C_n \frac{V(\Delta P)_{pp}^2}{8\gamma \overline{P}} \tag{B13a}$$

where the values of C_n and n are given in the following table:

C_n	n
0.861	1
.686	2
.610	3

Combining (B4), (B5), and (B13) gives the efficiency expression in terms of known or measurable quantities.

$$\eta = \frac{2\pi(\Delta f)_{0.707} C_n V(\Delta P)_{pp}^2}{8\gamma w_j \frac{\overline{P}RT_j}{m} \frac{\gamma}{\gamma - 1} \left[1 - \left(\frac{\overline{P}}{P_j}\right)^{\frac{\gamma-1}{\gamma}}\right]} \tag{B14a}$$

REFERENCES

1. Maslen, Stephen; and Moore, Franklin K.: On Strong Transverse Waves Without Shocks in a Circular Cylinder. J. Aeron. Sci., vol. 23, no. 6, June 1956, pp. 583-593.

2. Wieber, Paul R.: Acoustic Decay Coefficients of Simulated Rocket Combustors. NASA TN D-3425, 1966.

3. Phillips, Bert; and Morgan, C. Joe: Mechanical Absorption of Acoustic Oscillations in Simulated Rocket Combustion Chambers. NASA TN D-3792, 1967.

4. Morse, Philip M.: Vibration and Sound. Second ed., McGraw-Hill Book Co., Inc., 1948.

5. Buffum, F. G., Jr.; Dehority, G. L.; States, R. O.; and Price, E. W.: Acoustic Attenuation Experiments on Subscale, Cold-Flow Rocket Motors. AIAA J., vol. 5, no. 2, Feb. 1967, pp. 272-280.

NASA-Langley, 1968 —— 12 E-3870

"The aeronautical and space activities of the United States shall be conducted so as to contribute . . . to the expansion of human knowledge of phenomena in the atmosphere and space. The Administration shall provide for the widest practicable and appropriate dissemination of information concerning its activities and the results thereof."

—NATIONAL AERONAUTICS AND SPACE ACT OF 1958

NASA SCIENTIFIC AND TECHNICAL PUBLICATIONS

TECHNICAL REPORTS: Scientific and technical information considered important, complete, and a lasting contribution to existing knowledge.

TECHNICAL NOTES: Information less broad in scope but nevertheless of importance as a contribution to existing knowledge.

TECHNICAL MEMORANDUMS: Information receiving limited distribution because of preliminary data, security classification, or other reasons.

CONTRACTOR REPORTS: Scientific and technical information generated under a NASA contract or grant and considered an important contribution to existing knowledge.

TECHNICAL TRANSLATIONS: Information published in a foreign language considered to merit NASA distribution in English.

SPECIAL PUBLICATIONS: Information derived from or of value to NASA activities. Publications include conference proceedings, monographs, data compilations, handbooks, sourcebooks, and special bibliographies.

TECHNOLOGY UTILIZATION PUBLICATIONS: Information on technology used by NASA that may be of particular interest in commercial and other non-aerospace applications. Publications include Tech Briefs, Technology Utilization Reports and Notes, and Technology Surveys.

Details on the availability of these publications may be obtained from:

SCIENTIFIC AND TECHNICAL INFORMATION DIVISION

NATIONAL AERONAUTICS AND SPACE ADMINISTRATION

Washington, D.C. 20546